CHAPTER V
TOUGHENING OF POLYBENZOXAZINE BY SILK SERICIN-g-PLA/MARL BIOCOMPOSITES

5.1 ABSTRACT

Polylactide (PLA) is the most widely known biodegradable polymer in use today. Additionally, natural proteins in silk, sericin, have been increasingly used. This work emphasized the synthesis of a graft copolymer, Sericin-g-PLA, in the presence of surface treated marl as a filler, followed by blending with polybenzoxazine to harden the obtained biocomposite. Polybenzoxazine precursor was synthesized via the faster quasi-solventless approach with 88% yield. The synthesized polybenzoxazine precursor was blended with marl having surface modified by (3-aminopropyl) trimethoxy-silane. The chemical structures of the graft copolymer and polybenzoxazine precursor were confirmed by FTIR and NMR. The results of DSC showed that graft copolymer filled with modified marl can lower the curing temperature of polybenzoxazine, meanwhile; TGA results demonstrated the thermal stability increased as a function of graft copolymer contents. Regarding the effect of introducing graft copolymer on the mechanical properties of the biocomposite, particularly flexural and impact strength, it was observed that the biocomposite with 20 wt% graft copolymer added modified marl harden with polybenzoxazine gave the highest flexural strain and impact strength.

Keywords: Silk Sericin, Polylactide, Marl, Polybenzoxazine, Biocomposite

5.2 INTRODUCTION

Nowadays, there is a growing demand for biodegradable polymers. One of the major causes is the world-wide energy crisis. Also, environmental concerns have brought about the need for a more easily degrading material. Hence, polylactide (PLA), which is the most widely known biodegradable polymer in use today, is becoming more important. Additionally, natural glue-like proteins in silk, sericin, have

been increasingly used. However, products from the biopolymer, PLA, have some shortcomings and needs modification due to its brittleness. Introducing a low T_g polymer into the polymer backbone can impart flexibility to the PLA. For example, a copolymer can be obtained from the graft copolymerrization process. Previous works [4,28,44] successfully synthesized the graft copolymer of PLA with dextran and chitosan, which are natural polysaccharides. Nevertheless, low mechanical properties are still problems for practical uses.

Polybenzoxazine (PBZ) is a newly developed phenolic resin, with molecular design flexibility and good dimensional stability. Benzoxazine (BZ) monomers are typically synthesized by employing the solution method or the solventless method (melt-state process), through the Mannich condensation of phenol, formaldehyde, and amine. Many published researches about polybenzoxazine have targeted the improvement of the toughness of these materials. Ishida *et al.* [14–16] tried to reduce the brittleness of polybenzoxazine by blending it with poly (ε-caprolactone) and developing a new class of difunctional or multifunctional benzoxazine monomers by using bisphenol-A or diamine to conquer the limits of the product resulting from mono-functional benzoxazines, which gave only the oligomeric structure. Takeichi *et al.* [39] synthesized high molecular weight polybenzoxazine precursors from diamine and bisphenol-A, such that the crosslink polybenzoxazine film showed an improved toughness.

Marl, or white soil, contains more than 80% calcium carbonate, which can be used as a cool powder for anti-sweat, anti-infection, and skin disease reduction. Because of its advantages, marl, which is similar to calcium carbonate or clay, is chosen in this research to use as a filler to improve the mechanical properties and to lower the price of product, at the same time. However, because of its polar nature, it often requires surface treatment before incorporation into a non-polar plastic matrix. Better compatibility, achieved by different coupling agents, for example silanes and titanates, can be applied [3,14–15,27] to yield high mechanical properties of the composites, Moreover, much cheaper nonreactive coupling agents, such as fatty acids (mostly stearic acid) was successfully applied in calcium carbonate–polymer composites.[42] And from the previous work, it showed that the surface treated marl

can improve the conversion of benzoxazine monomer and mechanical properties of polybenzoxazine composites.

In this work, the sericin-g-polylactide copolymer filled with marl, so called biocomposite, was prepared via in-situ catalytic ring opening polymerization using a brabender mixer, and the newly developed quasi-solventless approach is used for synthesis the polybenzoxazine precursors with a faster reaction time by using 1,6-diaminohexane, bisphenol-A, and paraformaldehyde. Afterward, the marl filled graft copolymer was blended with the synthesized polybenzoxazine precursors at various ratios to optimize the mechanical properties of the final product.

5.3 EXPERIMENTAL

Materials

L-lactide monomer ((3*S*)-*cis*-3,6-Dimethyl-1,4-dioxane-2,5-dione) (99.5% in water) was supplied by Bio Invigor Corporation Co., Ltd. The silk sericin powder was supported by Chul Thai Silk Co., Ltd. Bisphenol-A (97%, purity) and 2-ethylhexanoic acid Tin (II) ($Sn(Oct)_2$) were supplied from Sigma Aldrich Chemical. Paraformaldehyde (98.7%, purify) was supplied from Merck. 1,6-Diaminohexane (99%, purify) and Lithium chloride (LiCl) were supplied from Fluka. The marl, or marly limestone, is a product from Lopburi Province, Thailand. The modifying agents, stearic acid ($CH_3(CH_2)_{16}COOH$) and silane coupling agent—(3-aminopropyl) trimethoxysilane, $NH_2(CH_2)_3Si(OCH_3)_3$—were purchased from Sigma Aldrich Chemical.

1,4-dioxane (AR grade) and ethyl acetate (AR grade) was supplied from Lab Scan Co., Ltd. Tetrahydrofuran (THF, HPLC grade) was purchased from Burdick&Jackson supplier (B&J). Methyl and Ethyl alcohol were purchased from Italmar. All chemicals are used without further purification.

Synthesis of Aliphatic Diamine Based on a Polybenzoxazine Precursor via the Quasi-Solventless Method

The polybenzoxazine precursor (shown in Scheme I) was prepared by reacting bisphenol-A (6 mmol) with a paraformaldehyde solution (24 mmol) in 1,4-dioxane at 10°C. The mixture was stirred continuously before a solution of 1,6-diaminohexane (6 mmol) in 1,4-dioxane was slowly added, and then it was stirred continuously until the solution formed a gel. The reaction temperature was then raised to 80–90°C; the mixture was continuously stirred for 1 h until a homogeneous yellow viscous liquid was obtained. The chemical structure of the precursors was confirmed by FTIR and ^{1}H NMR.

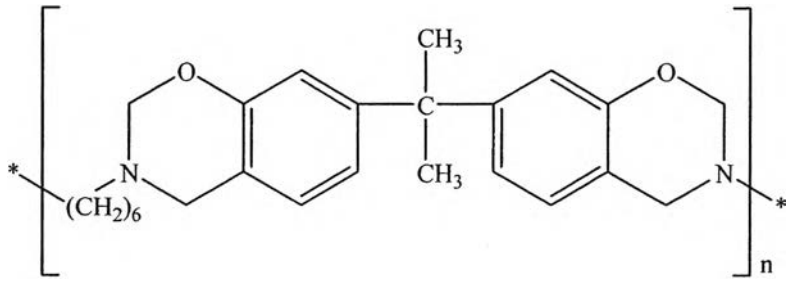

Figure 5.1 Schematic structure of the synthesized polybenzoxazine

Surface Modification of a Marl Filler

Surface modification of marl with amino silane was carried out in solution. An aqueous ethyl alcohol solution was prepared, and the silane coupling agent (1 wt% filler) was added to the solution, which was then mixed by a stirrer for 15 min. Afterwards, the sieved marl was added to the silane/water mixture and stirred for 2 h The solution was stirred continuously. When the set reaction time elapsed, the solution was dried under vacuum. The treated marl was pulverized and sieved again before used as the filler in a graft copolymer. The chemical analysis and morphology were obtained with FTIR and SEM, respectively.

Synthesis of a Silk Sericin Protein–Polylactide Graft Copolymer

The polymerizations were carried out under magnetic stirring for 24 h in dimethyl sulfoxide at 130°C. The sericin protein was dried in a vacuum oven at 70°C

for 24 h, after that it was dissolved in 10 ml of 1 M LiCl/DMSO by heating at 60°C for 60 min under nitrogen atmosphere. $Sn(Oct)_2$, which used as a catalyst for the ring-opening polymerization of lactide was added dropwise to the solution. The mixture was then stirred continuously for 4 h at the same temperature under nitrogen atmosphere. A solution of lactide in 10 ml DMSO was then placed into the sericin mixture (in the weight ratio of 20:80 (sercin/LA)). It was placed into a preheated oil bath, which was controlled at 130°C by a thermostat, stirred by a magnetic stirrer, and kept under nitrogen atmosphere. The reaction was allowed to proceed for 24 h. After 24 h had passed, the mixture became dark brown. The reactor was then cooled to room temperature. The mixture was precipitated by cold water (200 ml), and filtered out with a Buchner funnel for chemical analysis by FTIR spectrometer.

Synthesis of a Silk Sericin Protein–Polylactide Graft Copolymer with a Marl Filler by Using a Brabender Mixer W50

To conduct grafting from technique and ring-opening polymerization of lactide in bulk phase, the lactide monomer, marl filler, and sericin protein (at a weight ratio of sericin:LA:marl filler of 1:2:4) using $Sn(Oct)_2$ as a catalyst. The mixture was placed in a mixer chamber which was used as a polymerization reactor. First, 26 g marl and $Sn(Oct)_2$ were added to the chamber mixer and were mixed for 5 min at 100°C. Then the 6.5 g of silk sericin and 13 g of lactide monomer were added and mixed for a further 30 min. The processing conditions included a rotor speed of 50 rpm, an operating temperature of 130°C, and a monomer-to-catalyst with weight ratio of 0.1:100. The resulting polymers received from a Brabender Mixer were purified by soxhlet extraction with ethyl acetate at the temperature about 190°C for 3 h to remove both of lactide monomer and polylactide homopolymer. After that the resulting products were dried in vacuum oven at the temperature of 60°C before the chemical structure of graft copolymer was characterized by Fourier transform infrared (FTIR) spectroscopy and proton nuclear magnetic resonance (^{1}H NMR).

Preparation of the Biocomposite Material for Using as a Soft Splint from Sericin-g-PLA Blended with Polybenzoxazine

The graft copolymer filled with modified surface marl 2.2, 5.0, 8.6, 13.3, and 20 g, prepared in a brabender mixer, was dispersed in 1,4-dioxane 20 ml and stirred by homogenizer at a speed of 8000 rpm for 30 min. The homogenized solutions at various concentrations were added to the synthesized polybenzoxazine precursor at 80–90°C to obtain the biocomposite of graft copolymer in polybenzoxazine between 10–50 wt%, and a homogeneous solution was obtained after thorough mixing. The mixture was preheated at 80–100°C for solvent removal followed by step-cured in a compression molding (Wabash, model V50H-18-CX) at a force of 20 ton to be a thin sheet with 3 mm thickness. The polymerization temperature profile for compression molding process of polybenzoxazine and biocomposites were obtained at 80, 100, 120, 150, 180, and 200°C. The biocomposite sheets were cut into the specific sizes and were characterized by FTIR, DSC, TGA, SEM, DMA, flexural, and tensile testing.

Characterization

The presence of functional groups of polymers was determined by using an FTIR Nicolet Nexus 670 spectrometer in the frequency range of 4000–400 cm^{-1} with 32 scans at a resolution of 4 cm^{-1} by using a KBr pellet technique. Proton Nuclear Magnetic Resonance (NMR) spectra were recorded on a Varian Inova 500 NMR working at 500 MHz. The morphology was studied by scanning electron microscopy (JEOL JSM-5410) at 15 kV. The thermal stability was investigated by differential scanning calorimerty (DSC) using a Perkin-Elmer DSC 7 instrument by heating the samples from 50–400°C at a rate of 10°C/min under a N_2 atmosphere with a flow rate of 20 ml/min and thermal decomposition temperatures were observed with a Mettler TGA (Thermogravimetric analysis) instrument. The samples were heated from 50–850°C at a heating rate of 10°C/min under a N_2 flow of 50 mL/min. Dynamic mechanical analysis (DMA) were obtained with a dynamic-mechanical analyzer NETZSCH DMA 242 instrument. The specimens with dimensions of approximately 60×10×3 mm^3 were tested in a rectangular torsion fixture. A sinusoidal shear

strain of 0.1% was applied at a frequency 1 Hz during each temperature sweep experiment. Linearity of the chosen shear strain was verified by a strain sweep prior to each experiment. Measurement were collected every 2°C as the samples were heated at a rate of approximately 3°C/min from -100°C to well above the glass transition of each material. X-ray diffractometer (XRD) was used to investigate the crystal structure of a graft copolymer. XRD patterns were measured on a Bruker AXS Model D8 Advance. The X-ray beam was Ni-filtered Cu K_α operated at a tube voltage of 40 kV and a tube current of 30 mA. The powder samples were observed on the 2θ range of 2–80 degree with a scan speed 2 degree/min and a scan step 0.01 degree.

Flexural testing was performed using an Instron/4206 Universal Testing Machine (UTM). The flexural specimens were prepared according to ASTM D790M. The UTM was fitted with a 5 kN static load cell and a standard 3-point bending fixture. Flexural test specimens, with dimensions of 60×10×3 mm^3, were tested for each material using the Series IX control and analysis software. The samples were flexed until breakage at a rate 1.28 mm/min using a support span of 48 mm. Flexural strain was calculated based on crosshead movement. The flexural stress, modulus, and strain were reported from at least five average values. The impact testing was performed by cutting sheets of sample into the specimen shape following the ASTM D256 (notched IZOD type) with dimensions of 64×12.7×3.2 mm^3, then the impact strength were tested by the ZWICK impact testing machine with the pendulum load of 2.7 J. The impact strength was reported from at least five average values.

The molecular weight and molecular weight distribution were measured by Gel Permeation Chromatography (GPC) Shimadsu Model, which was carried out in water solvent as the mobile phase using PL aquagel-OH 50 8 μm Column and RID-10A detector. The water solvent was filtrated with MN 615 ∅ 155 mm filter paper under the vacuum. The crude graft copolymers were dissolved in water at the concentration 0.5 wt% and filtrated with 0.45 mm diameter of cellulose acetate filter before injecting into the column. The conditions of this machine were 40°C column temperature, 1 ml/min flow rate, and 30 min run time. Molecular weight and molecu-

lar weight distribution of graft copolymer were calculated employing a PL Pollutant Calibration kit (PL), as shown in Figure 5.2.

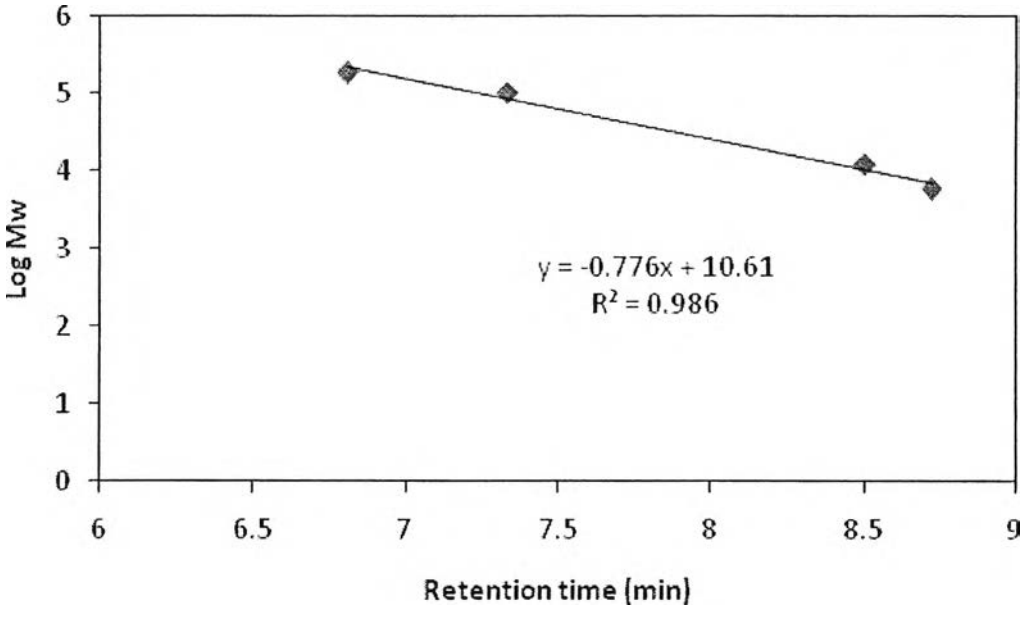

Figure 5.2 The PL pollulant calibration for the calculation of molecular weight.

5.4 RESULTS AND DISCUSSION

5.4.1 Preparation of the Polybenzoxazine Precursors

The synthesis of precursors is based on the Mannich reaction of bisphenol-A, 1,6-Diaminohexane, and paraformaldehyde at the molar ratio of 1:1:4 via a quasi-solventless approach. The functional groups of the synthesized polybenzoxazine were confirmed by FTIR, as shown in Figure 4.4. The ^{1}H NMR spectrum proved that polybenzoxazine had been successfully synthesized (see Figure 4.5). The better points of this method include the completing reaction time is less than the traditional method with an obtained high molecular weight precursors at a comparable yield.

5.4.2 Surface Modification of a Marl Filler

The weak interfacial adhesion between the surface of the marl and polybenzoxazine as shown by the SEM micrographs (Figure 4.12) suggested the necessity for compatibility improvement, by using the silane coupling agent. The chemical structure of treated marl was confirmed by FTIR spectra that coupling agents were bounded to the marl by using this treatment method.

5.4.3 Synthesis and Characterization of a Silk Sericin Protein-Polylactide Graft Copolymer

5.4.3.1 Chemical Analysis of the Graft Copolymer

The sericin-polylactide grafting copolymers were prepared either by using glassware and brabender mixer. Structural changes of sericin and its graft copolymer were confirmed by FTIR spectra, as shown in Figure 5.3. Compared to the IR spectrum of sericin, the copolymers had a new absorption peak appearing around 1762 cm^{-1}, corresponding to the ester carbonyl group of the branched polylactide. The methyl asymmetric deformation of polylactide appeared at 1454 cm^{-1}. The 1272 cm^{-1} singlet observed in the copolymer was assigned to the asymmetric C–O–C stretching of the ester groups. There were two peaks, at 1133 and 1053 cm^{-1}, attri-

buted to the methyl rocking and C–CH_3 stretching vibration, respectively. This evidence suggested that lactide could indeed react with silk sericin. The peak at 3300 cm^{-1} belonged to the hydroxyl group. The amino peak and the amide peak of silk sericin did not shift remarkably after the copolymerization. An increase in the observed amide peak (1662 cm^{-1}) indicated the formation of amide linkage during the grafting reaction ((Luckachan *et al.*, 2006) and (Wu *et al.*, 2005). The grafting reaction between silk sericin protein and lactide monomer was shown in Figure 5.4.

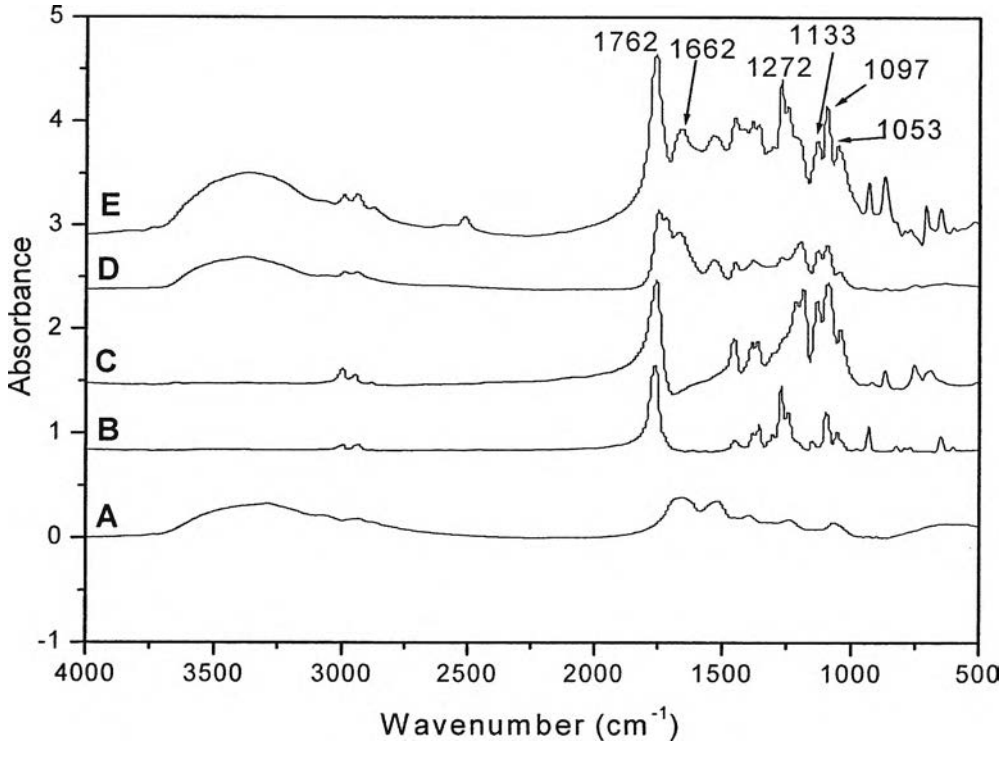

Figure 5.3 FTIR spectra of polylactide, sericin, and graft copolymer: (A) sericin, (B) lactide monomer, (C) polylactide, (D) Ser-g-PLA in glassware, and (E) Ser-g-PLA in brabender.

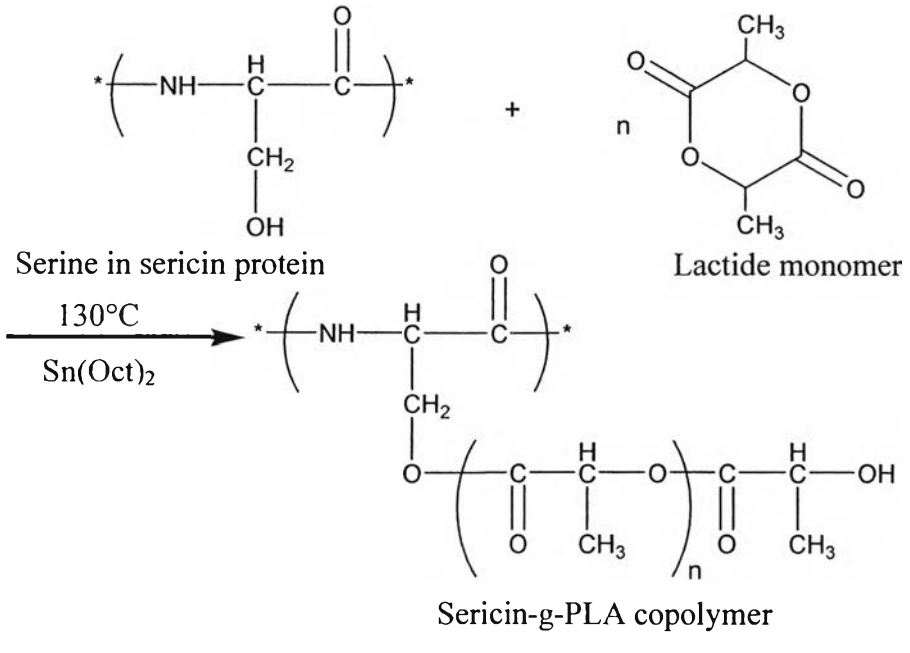

Figure 5.4 Reaction scheme for grafting copolymerization of silk sericin protein and lactide monomer. *(**Note** an asterisk for both sides of sericin refered to 18 amino acids, i.e. serine; glycine;, tyrosine; glutamine, which could bond to lactide grafted serine.)*

The ^{1}H NMR spectra of the grafted copolymer were shown in Figure 5.5 (b). Silk sericin should show the proton peaks at 6.68 and 6.96 ppm (Cho *et al.*, 2003) of the tyrosine residue. The results indicated that the signal shifted downfield to 6.80 and 7.10 ppm, respectively, which suggested the change in the molecular environment of the tyrosine residue caused by the modification. While polylactide showed the peak at 1.56 ppm, which was attributed to the methyl groups (–CH_3). The peaks at 4.43 and 5.25 ppm were assigned to terminal methine (–CH–) protons of the branched polylactide and its repeating units in the chain, respectively. Both signals were clearly separated into two groups of protons. This implied that there were two different kinds of atoms bonding to the methine. The stronger intensity signal of 4.93 ppm corresponded to the methine protons which bonded to silk sericin chain, (–NH–CH–CH_2–), hence it confirmed the occurrence of synthesized graft copolymer (Liu *et al.*, 2004).

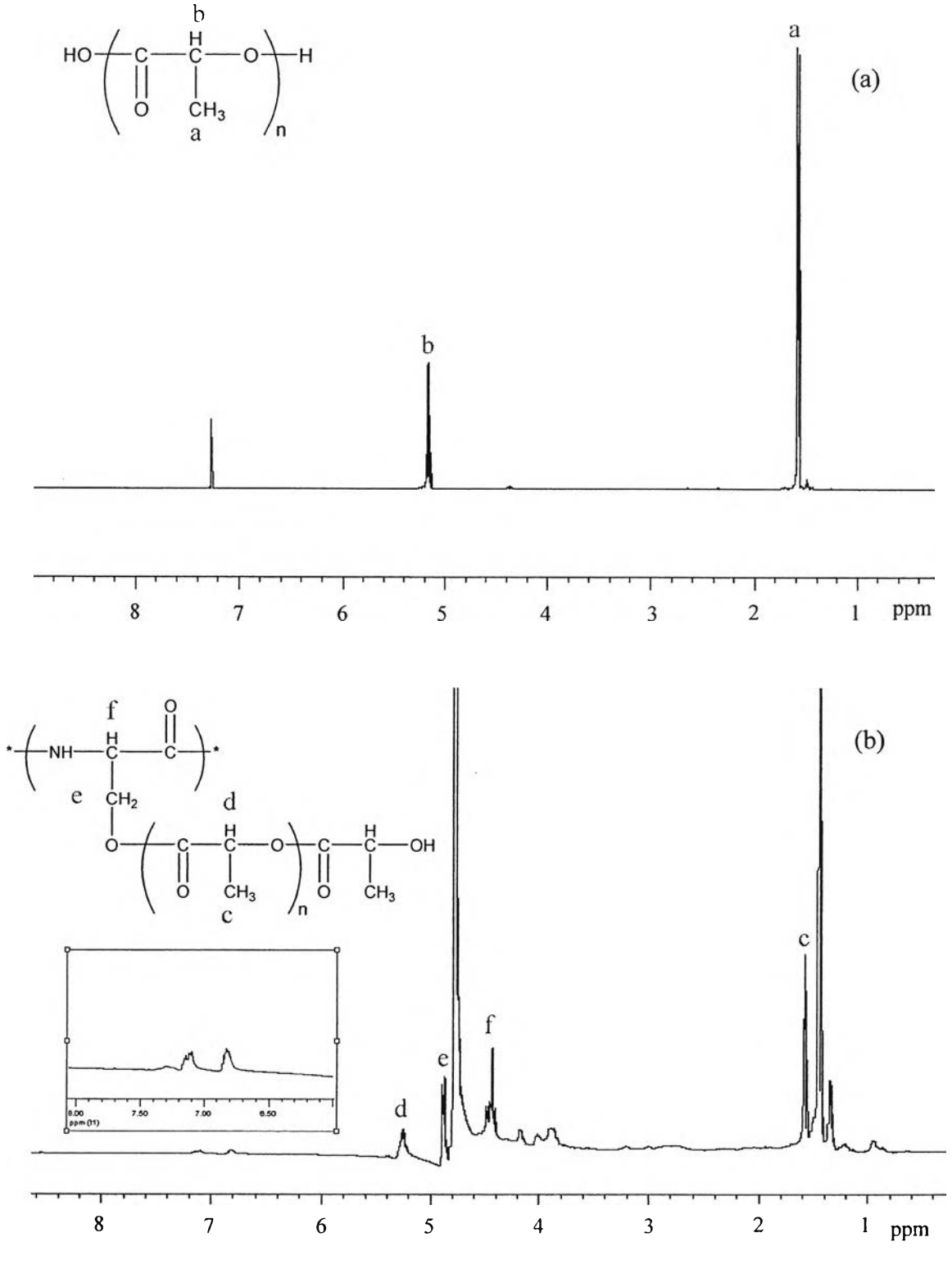

Figure 5.5 ^{1}H NMR spectra of (a) synthesized polylactide at 130°C in $CDCl_3$, and (b) surface modified marl filled silk sericin-polylactide graft copolymer prepared by brabender mixer at 130°C in D_2O.

5.4.3.2 Thermal Analysis of the Graft Copolymer

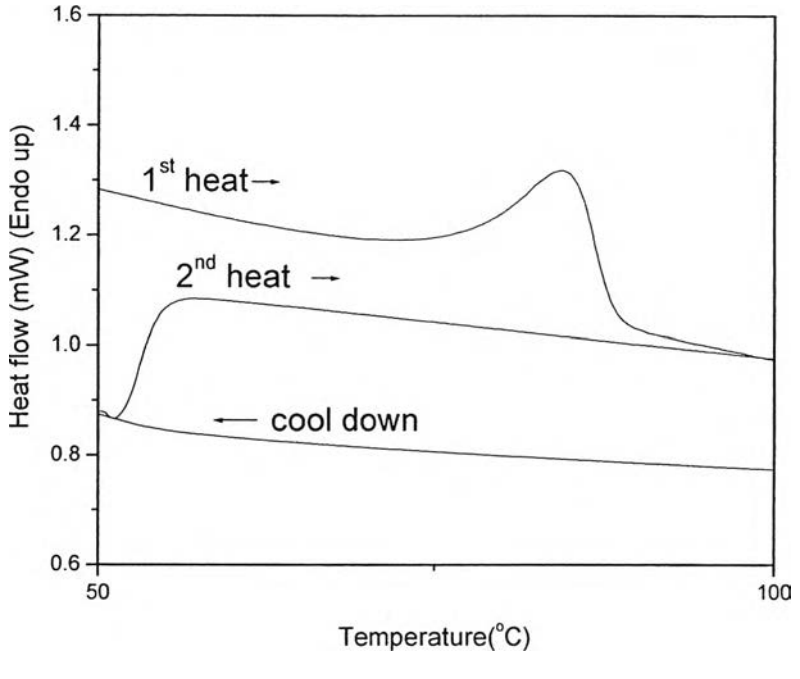

Figure 5.6 The DSC curves of the crude synthesized modified marl filled silk sericin-polylactide graft copolymers.

The DSC curve of a graft copolymer prepared in a brabender mixer was illustrated in Figure 5.6. The first heat of graft copolymer shows a little endothermic peaks at 86.5°C, lower than lactide monomer and PLA polymer (see in Table 5.1), and the crystallization of PLA phase did not occur after grafting from silk sericin backbone. In addition, the thermal stability of Sericin-g-PLA added modified surface marl was examined by TGA measurement and the weight loss was taken in Table 5.2. The decomposition temperature of graft copolymer was approximately 216°C, as observed from Figure 5.7, which was higher than reactants; lactide and sericin.

Table 5.1 The melting temperature (T_m) and crystallization temperature (T_c) of lactide, polylactide, and the graft copolymer

Material	T_m(°C)		T_c(°C)	
	Onset	Peak	Onset	Peak
Lactide monomer	94.21	97.17	-	-
Polylactide	164.96	172.00	108.52	98.63
Ser-g-PLA	78.85	86.50	-	-

Table 5.2 Thermal properties of the synthesized graft copolymer compared to the pure reactants

Samples	T_d onset (°C)		Weight Loss	Char Residue
	Peak 1	Peak 2	(%)	(wt%)
Lactide monomer	187.15	-	96.9	3.1
Synthesized PLA	319.1	-	95.3	4.7
Sericin	199.8	-	86.5	13.5
Marl	718.8	-	38.5	61.5
Graft copolymer	215.9	728.8	64.6	35.4

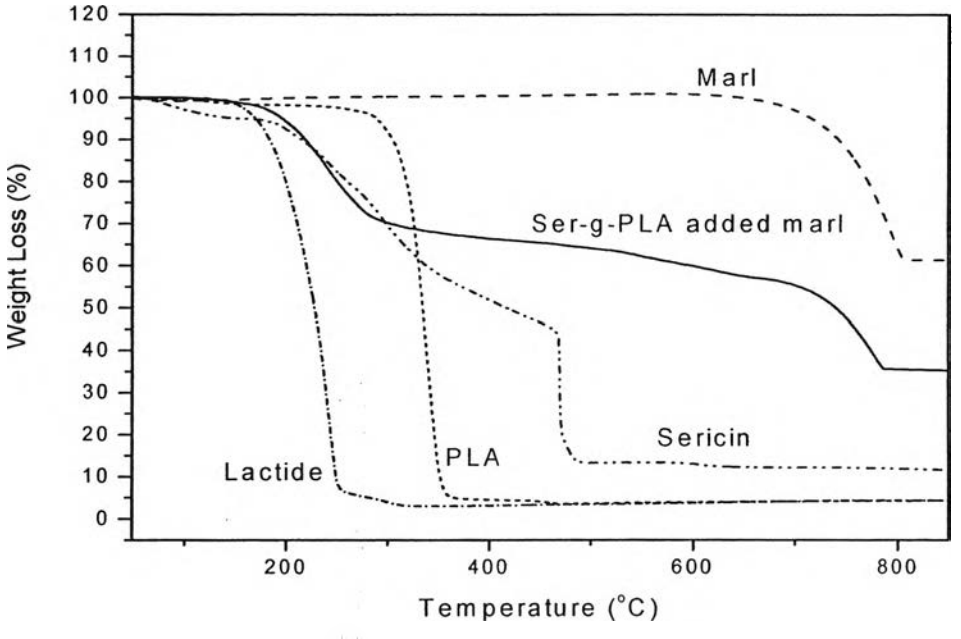

(a)

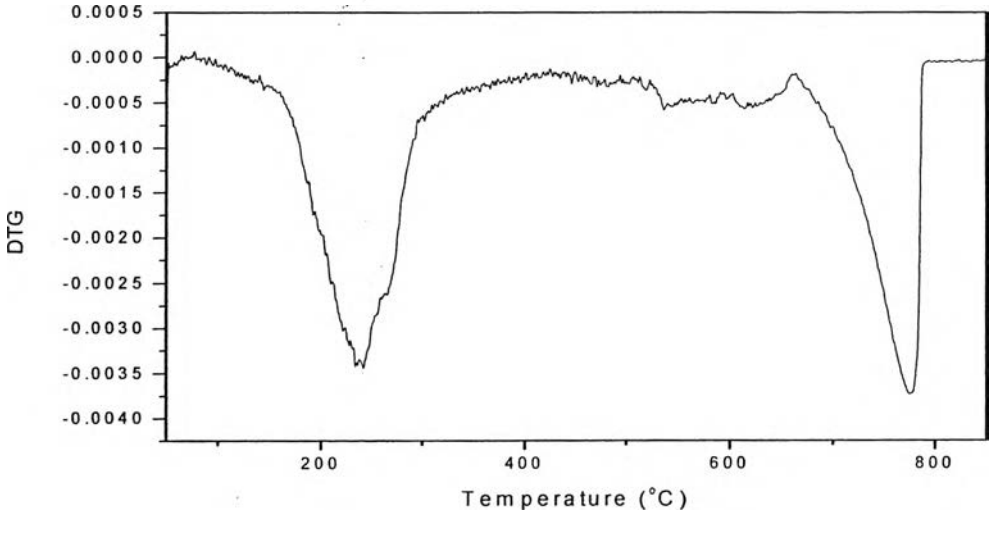

(b)

Figure 5.7 TG-DTA plots of the surface modified marl filled silk sericin-polylactide graft copolymer: (a) weight losses of the sample and (b) differential weight loss (DTG) curve. Percent weight loss of the synthesized polylactide, sericin, lactide monomer, and marl are also noted for comparison.

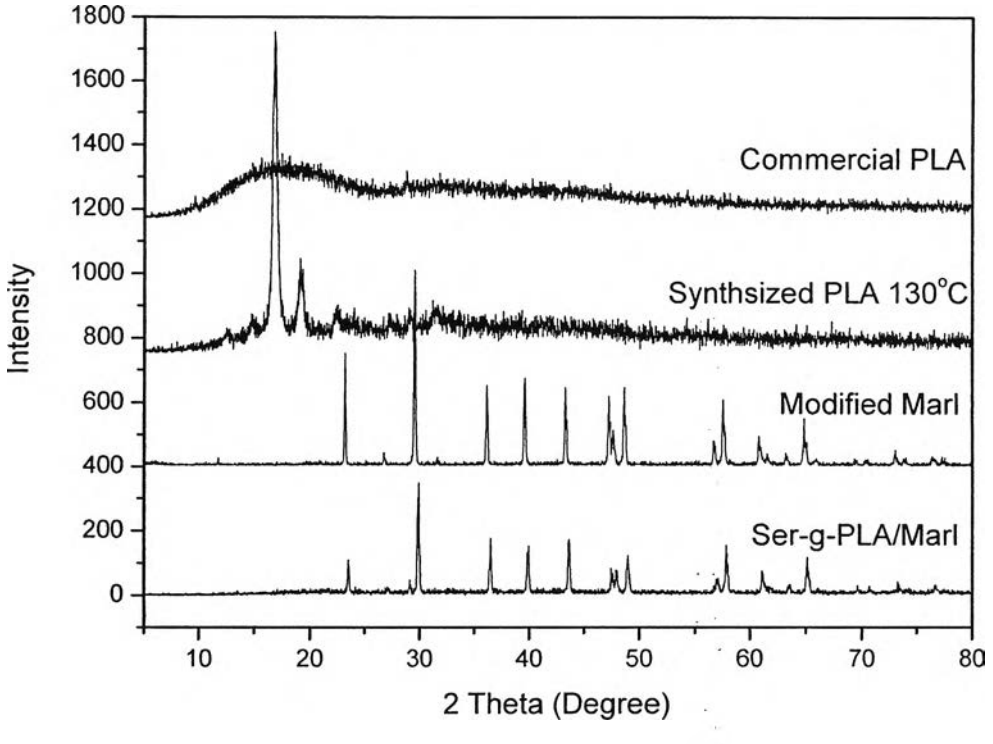

Figure 5.8 XRD patterns of crude sericin-g-PLA added modified surface marl produced in brabender mixer with 0.1 wt% $Sn(Oct)_2$, and 50 rpm screw speed. XRD patterns of the synthesized polylactide, commercial polylactide, and marl are also noted for comparison the cystallinity.

Figure 5.8 shows the X-ray diffraction patterns of polylactide and its graft copolymer filled with marl. Pure PLA in commercial grade exhibits a broad crystalline peak at 16.7° 2θ which is identical to a strong sharp peak of synthesized PLA (at temperature of 130°C, in toluene solvent), whereas the surface modified marl exhibits the peaks in 2θ Bragg angle with such values as 23.2, 36.0, 39.5, 43.5, 47.5, 48.5 and the strongest peak at 29.5 corresponding to the calcite phase of calcium carbonate polymorphs (Chirstos and Nikos, 2000). For the curves of the graft copolymer, it had the decreasing intensity peak at positions of 23.7, 30.0, 36.5, 40.0, 44.0, 48.0, and 49.0 , which are slightly shifted from modified marl pattern. The comparison of X-ray dif-

fraction profile of pure PLA, surface modified marl, and modified marl added graft copolymers indicated that the grafting had destroyed the original crystallization of pure PLA and changed the original molecular structure of marl (Liu *et al.*, 2004). The XRD result of graft copolymer confirmed that the endothermic peak of the first heat scan from DSC (at 86.5°C) should be the melting temperature of small molecules that remained in the crude product of graft copolymer.

5.4.3.3 Molecular Weight Measurement

Molecular weight, molecular weight distribution, and the purity of the resulting polymers were measured by using the gel permeation chromatography (GPC). GPC was carried out in water using a PL aquagel-OH water column with a reflactometer index detector. Molecular weight and molecular weight distribution of these polymers were calculated in reference to a following polystyrene calibration:

$$\log M = -0.77609065T_r + 10.61316334 \quad (4)$$

Dispersion = 0.718576

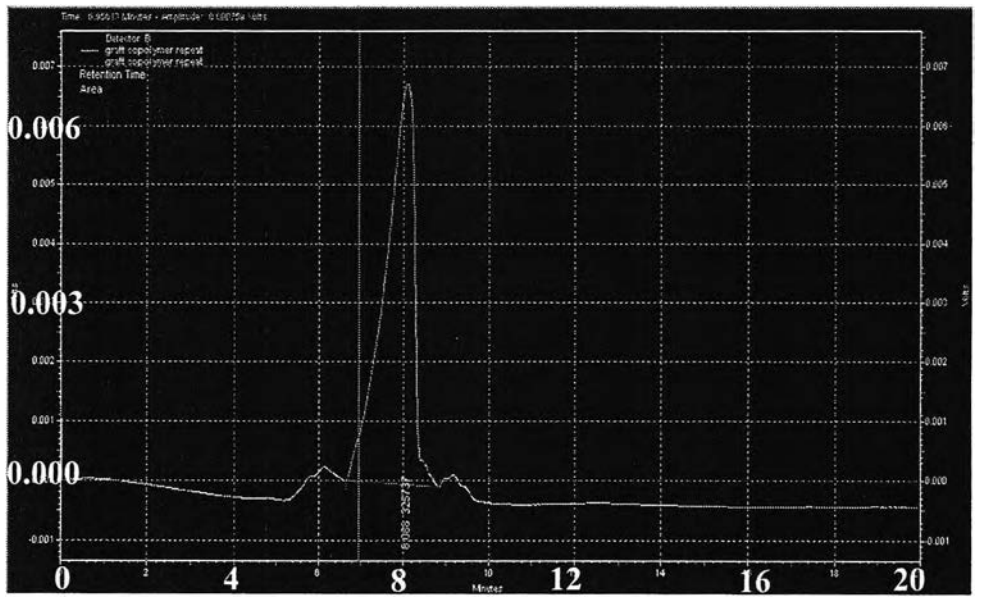

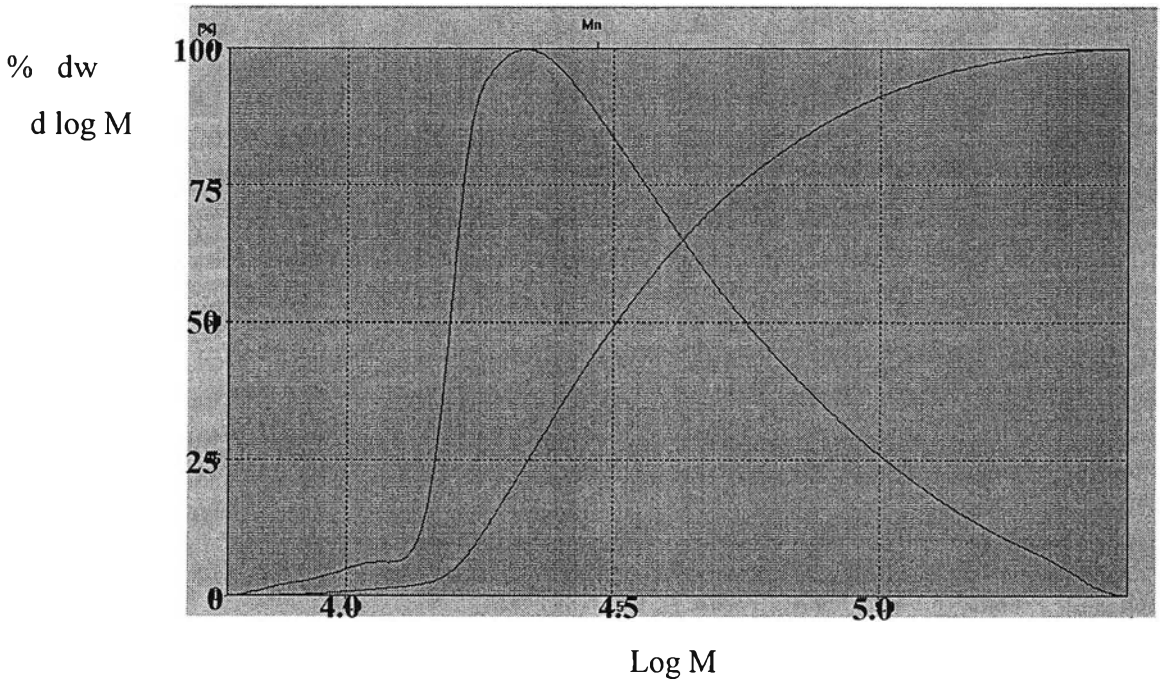

Figure 5.9 GPC curve for the modified surface marl filled silk sericin-polylactide graft copolymer. With sample concentration of 0.5 wt% in water eluent, PL aquagel-OH 50 8μm Column, (7.5*300 mm), RID-10A detector, 40°C column temperature, 1 ml/min flow rate, and 30 min run time.

From GPC result, a single unimodal peak with no peaks of the corresponding homopolymer often formed as by-products in grafting was observed. The characteristic peak identified the obtained graft copolymer not being contaminated by polylactide homopolymer. After calculation the graft copolymer showed the weight average molecular weight (M_w) in the range of 48,360–61,583 and the number average molecular weight (M_n) in the range of 33,353–36,500, showing that its molecular weight was quite high when compared with 6,800 of graft copolymer from dextran and polylactide (Cai *et al.*, 2003). Additionally, it indicated that the structure of the obtained copolymer could be regarded as branched architecture since the content of silk sericin was lower than the majority units of lactide.

5.4.4 Preparation of the Biocomposites from Modified Surface Marl Filled Sericin-g-PLA Hardened with Polybenzoxazine

5.4.4.1 Preparation and Characterization of the Biocomposites

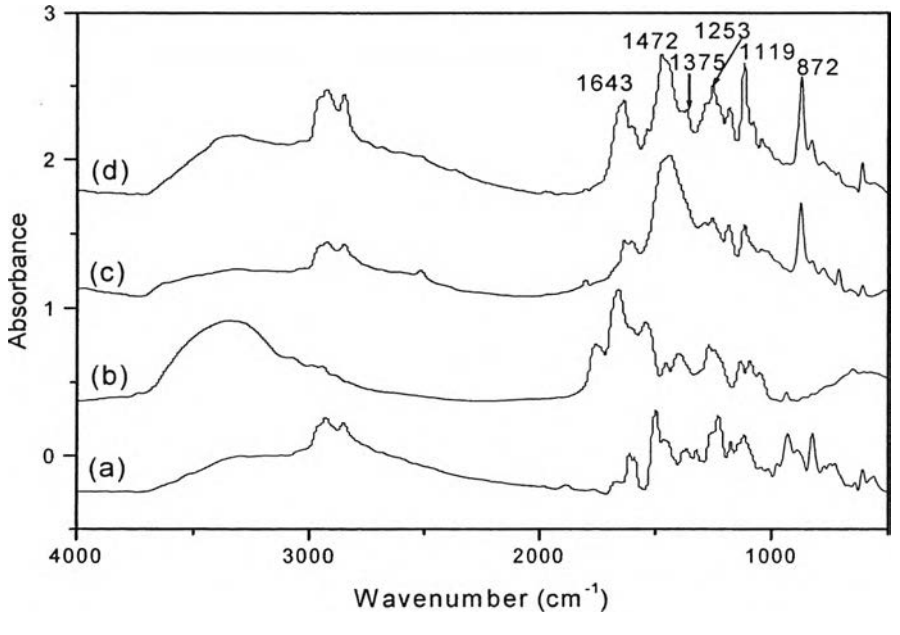

Figure 5.10 FTIR spectra of polybenzoxazine and its biocomposite: (a) polybenzoxazine after curing at 80°C, (b) Sericin-g-PLA added modified-surface marl, (c) biocomposite after curing at 200°C, and (d) biocomposite after curing at 80°C.

The graft copolymer added marl filler was blended with synthesized polybenzoxazine by solution blending at the various ratios and the resulting biocomposites were fabricated by using a compression molding technique. The functional groups of the obtained biocomposite from graft copolymer hardened by polybenzoxazine–marl were confirmed by FTIR, as shown in Figure 5.10. The characteristic bands of the benzoxazine precursor were at 1253, 1183, and 1375 cm^{-1}, corresponding to the asymmetric stretching of the C–O–C group, the asymmetric stretching of the C–N–C, and CH_2 wagging, respectively. Additionally, trisubstituted benzene rings at 1472 cm^{-1} and out–of–plane bending vibrations of C–H at 872 cm^{-1} were observed. The graft copolymer showed the characteristic peak at 3300, 1119, and 1043 cm^{-1} belonging to the hydroxyl group, methyl rocking, and C–CH_3 stretching vibration, respectively. The broadening hydroxyl peaks may imply the occurrence of hydrogen bonding between the polymer chains. The amide linkage peak at 1643 cm^{-1} confirmed the obtained graft copolymer in the biocomposite.

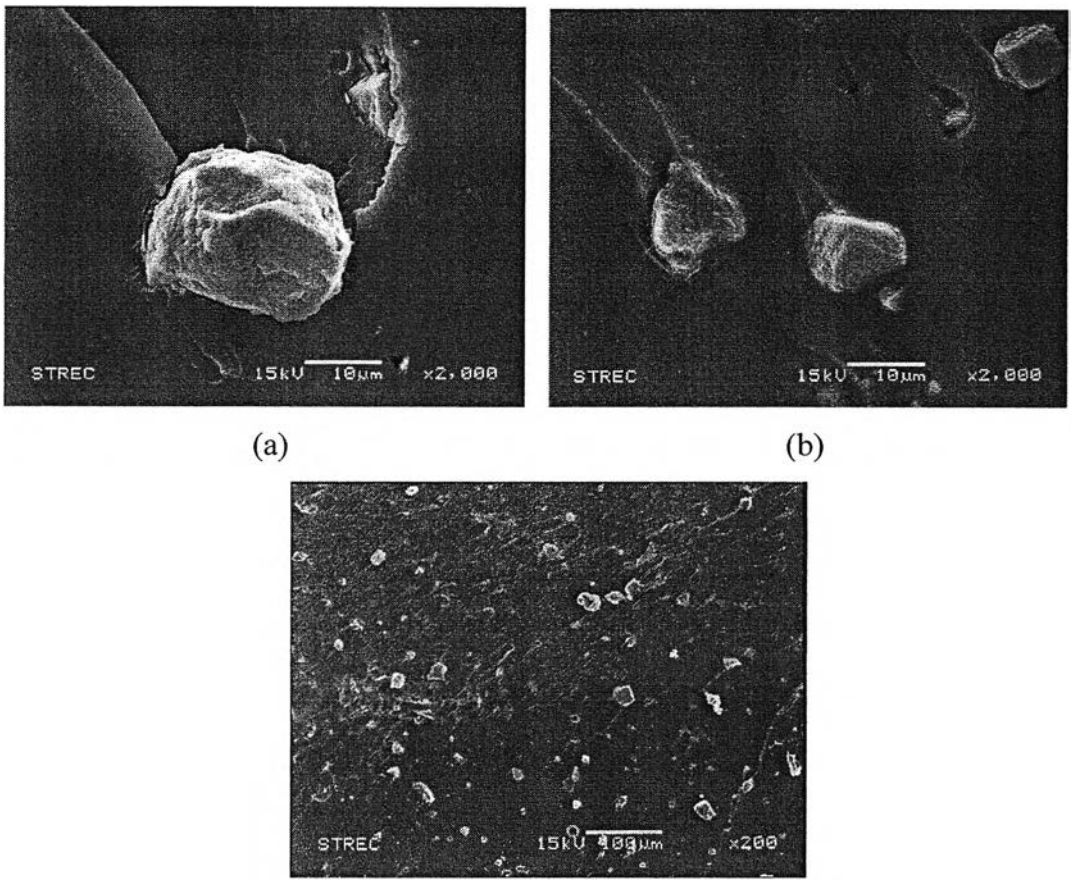

Figure 5.11 SEM micrographs of the fracture surface of the biocomposites (20 wt% graft copolymer) (a), (b) 2000x and (c) 200x.

The morphology of the biocomposites from a graft copolymer filled with modified-surface marl was studied by examining the fracture surfaces of the biocomposites by SEM, as shown in Figure 5.11. It was clearly observed that graft copolymer and amino silane-treated fillers were well embedded in the polybenzoxazine with the matrix covering around and on the fillers. These figures are the evidence of the bonding between graft copolymer, marl, and the polybenzoxazine matrix without the agglomeration of the filler particles. Figure 5.11(c) and 5.12 confirmed the good dispersion of marl in polymer matrix, but in Figure 5.12(c) the voids generated during compression molding process are clearly seen too. Those voids corresponded to the solvent left from the synthesis, resulted in the poor mechanical properties at the last.

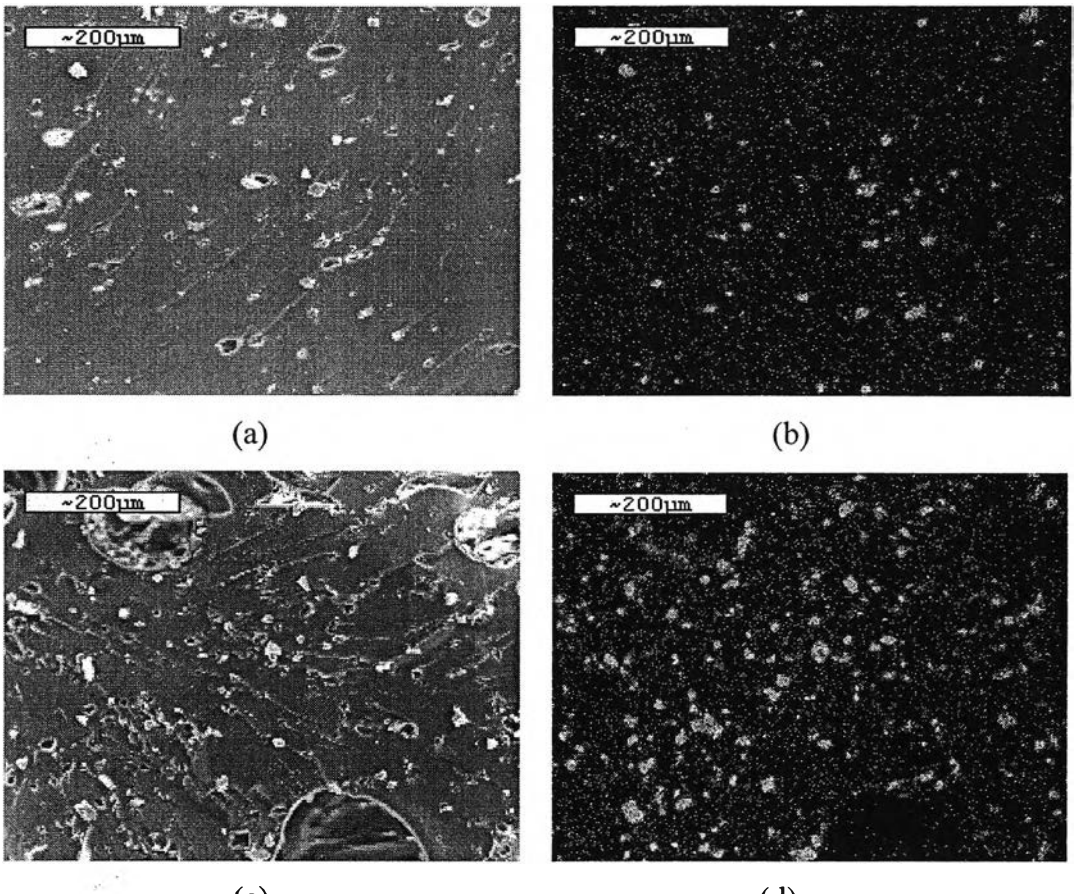

Figure 5.12 SEM images and their corresponding EDX micrographs of polybenzoxazine–biocomposite: (a) 10 wt% graft copolymer-marl with Ca mapping, (b) 10 wt% graft copolymer-marl SEM image, (c) 30 wt% graft copolymer-marl with Ca mapping, and (d) 30 wt% graft copolymer-marl SEM image.

5.4.4.2 Thermal Analysis of Biocomposites

The DSC thermograms of the heating scans were recorded for 10–50 wt% graft copolymer compositions in the polybenzoxazine precursors are shown in Figure 5.13(a) and summerized values of curing temperature and enthalpy in Table 5.3. The table shows that the onset temperatures of the exotherms of the biocomposites tend to decrease with increasing content of the graft copolymer and all the cured temperature of polybenzoxazine with graft copolymer are lower than that of the neat polybenzoxazine. This effect may arise from marl, which Takeichi *et al.,* 2006 believed that the acidic protons from silica in the marl functioned as an acid catalyst

to shift the onset of the ring opening process to the lower temperature. However, the curing content of polybenzoxazine increases after blending with graft copolymer due to the hydrogen bond occurred between polybenzoxazine and graft copolymer, which resulted of a higher crosslinking structure.

Table 5.3 Curing temperature and enthalpy of the polybenzoxazine biocomposites after solvent removal by drying in an oven at 80°C for 72 h

Composition (wt%)			Curing temp(°C)		ΔH (J/g) of	ΔH (J/g) of
Ser-g-PLA	PBZ	Marl	Onset	Peak	PBZ	PBZ (100 wt%)[a]
0	100	0	153.8	250.8	273	273
4.3	90	5.7	138.2	251.2	381	423
8.6	80	11.4	125.4	225.0	288	360
12.9	70	17.1	140.4	240.0	352	503
17.1	60	22.9	133.0	236.2	261	425
21.4	50	28.6	131.7	234.7	317	634

[a]ΔH of PBZ (100 wt%)= (ΔH of PBZ*100)/%PBZ.

Additionally, the progress of ring-opening polymerization of the pre-cursors was monitored by DSC in Figure 5.13(b) can verify the result of FTIR spectrum in Figure 5.10. By the end of 200°C cure, IR spectrum shows the decreasing characteristic absorption bands due to the opening cyclic benzoxazines, at 1253 cm^{-1} (asymmetric stretching of C–O–C of oxazine), at 1183 cm^{-1} (asymmetric stretching of C–N–C), at 1375 cm^{-1} (CH_2 wagging), at 1472 cm^{-1} (stretching of trisubstituted benzene ring) and at 872 cm^{-1} (out of plane bending vibrations of C–H). Meanwhile; the DSC thermograms of the biocomposites(see Figure 5.12b) showed that the exothermic peak completely disappeared after 200°C, which means that the ring opening of oxazine ring was completed. The need of fully cured polybenzoxazine because the fraction of H-bonded carbonyl groups increased dramatically with degree of curing,

since the free hydroxyl groups were produced through the ring-opening polymerization of benzoxazine.

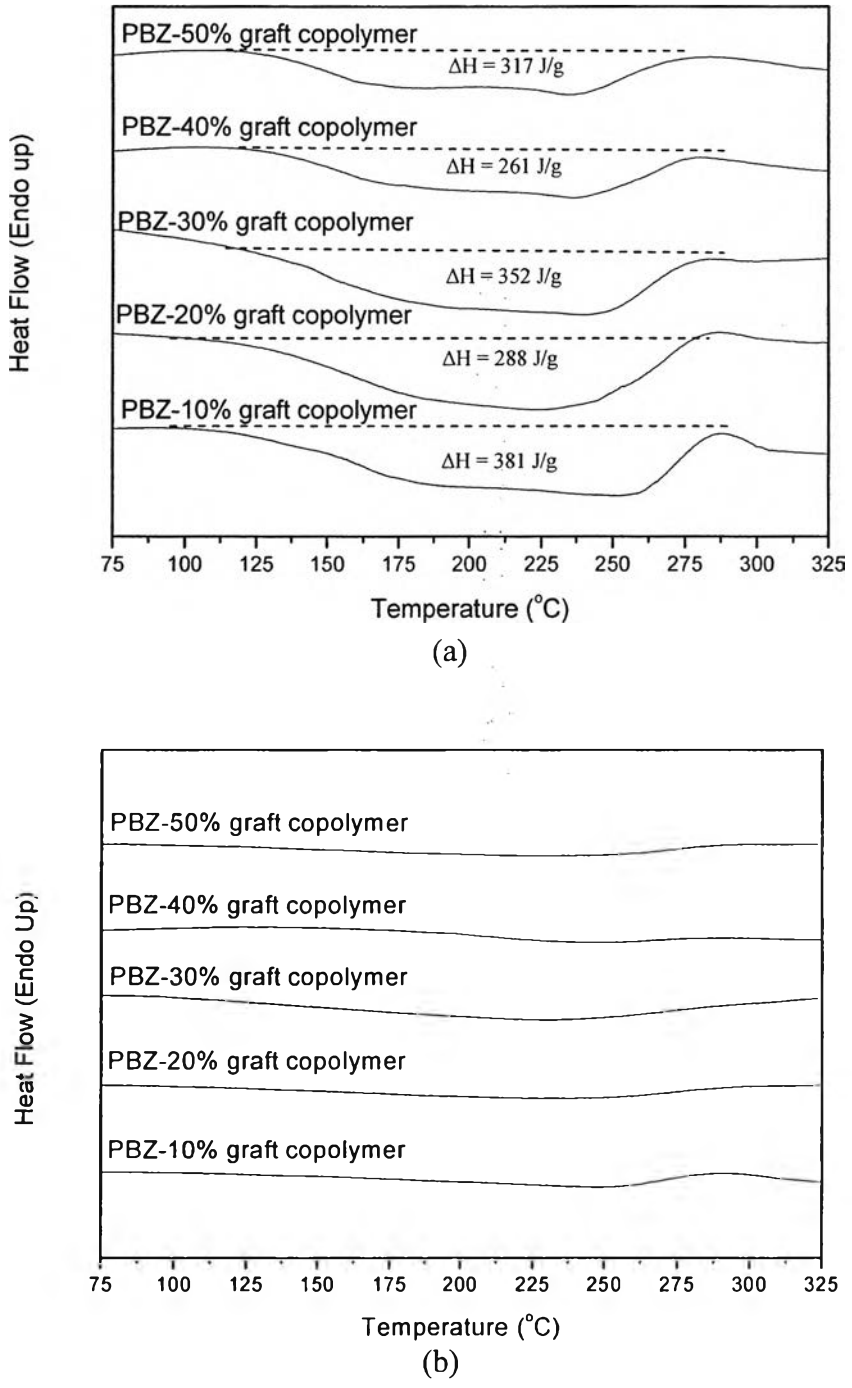

Figure 5.13 DSC of the biocomposites as a function of graft copolymer content: (a) uncured (at 100°C) and (b) fully cured (at 200°C).

Table 5.4 Thermal properties of the polybenzoxazine biocomposites (thermal properties of the synthesized polybenzoxazine and a graft copolymer are also noted for comparison)

Composition (wt%)			T_d onset (°C)		Weight Loss	Char Residue
Ser-g-PLA	PBZ	Marl	Peak 1	Peak 2	(%)	(wt%)
0	100	0	203.7	384.9	81.9	18.1
4.3	90	5.7	235.5	361.8	72.9	27.1
8.6	80	11.4	229.0	356.1	70.5	29.5
12.9	70	17.1	252.1	361.1	63.3	36.7
17.1	60	22.9	237.9	358.9	58.9	41.1
21.4	50	28.6	294.9	391.0	50.8	49.2
42.9	0	57.1	215.9	728.8	64.6	35.4

The thermal stability and char residue of the biocomposites were investigated by TGA, as shown in Figure 5.14. The TGA results, which are listed in Table 4.4, show the values of the biocomposite decomposition temperatures were higher than both of synthesized polybenzoxazine and graft copolymer, which are derived from the hydrogen bonding formation between the hydroxyl groups of polybenzoxazine and the carbonyl groups of polylactide graft copolymer (Ishida and Lee, 2001).

Also the char yield systematically increases with graft copolymer content from approximately 27% to 49% revealing the strong interaction between graft copolymer and PBZ. The behavior of biocomposite degradation remained two-stage weight-loss of the degradation process like that of the polybenzoxazine for low content of ser-g-PLA/marl. This agrees with the previous work by Allen *et al.*, 2006 who suggested that the first lower temperature weight loss process appeared to be associated with the degradation at the Mannich bridge and an associated loss of amine-related compounds, while the second higher temperature weight loss process was related to the phenol and aliphatic-related compounds.

However at high biocomposite contents (30–50 wt%), the decomposition was occurred as single step instead suggesting more intense of reaction between two components, as confirmed by FTIR (the broadening peak of N–H and O–H peaks). The single transition appeared at the decomposition of phenolic group; i.e. no small molecule was decomposed, which suggested that the strong intermolecular forces were introduced by the reaction of polybenzoxazine with graft copolymer.

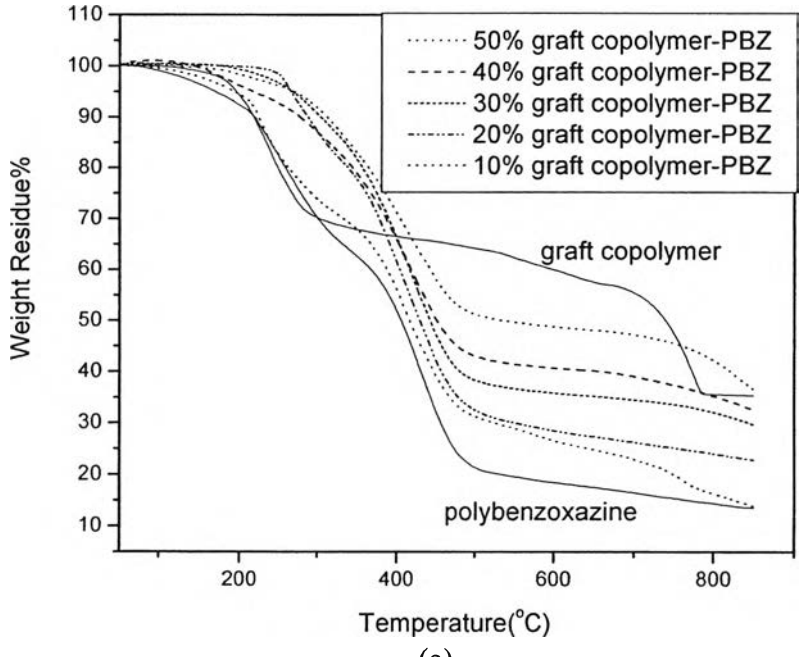

(a)

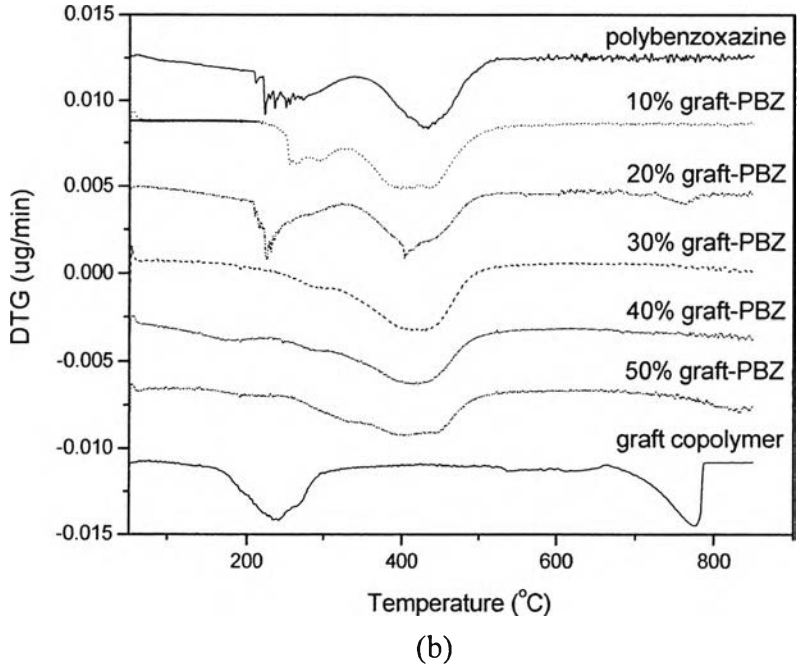

(b)

Figure 5.14 TG-DTA of the biocomposites as a function of a graft copolymer content: (a) weight losses of the sample and (b) differential weight loss (DTG) curve. Percent weight loss of the graft copolymer filled marl and the polybenzoxazine are also noted for comparison.

5.4.4.3 The Mechanical Properties of the Biocomposites

In this reserach the mechanical properties were determined by means of flexural properties and impact strength of the biocomposites, which were tested in accordance with ASTM specifications and are summarized in Table 5.5. The flexural strain, flexural stress, flexural modulus of elasticity, and impact strength are shown in Figures 5.15 to 5.18, respectively.

Table 5.5 Summary of the flexural properties and impact strength of the biocomposites

Composition (wt%)			Flexural testing			Impact strength (kJ/m^2)
Ser-g-PLA	PBZ	Marl	Strain (%)	Stress (MPa)	Flexural modulus (MPa)	
0	100	0	2.1±0.6	13.4±4.1	527.0±23.4	1.2±0.1
4.3	90	5.7	1.4±0.4	8.9±3.8	962.0±149.8	1.2±0.2
8.6	80	11.4	3.3±0.6	16.4±4.0	894.0±281.4	3.7±0.2
12.9	70	17.1	2.8±0.3	25.7±4.6	1381.8±221.9	2.4±0.3
17.1	60	22.9	2.8±0.7	26.7±5.3	1420.8±269.1	1.7±0.4
21.4	50	28.6	1.0±0.3	28.6±2.8	1732.6±178.6	1.5±0.5

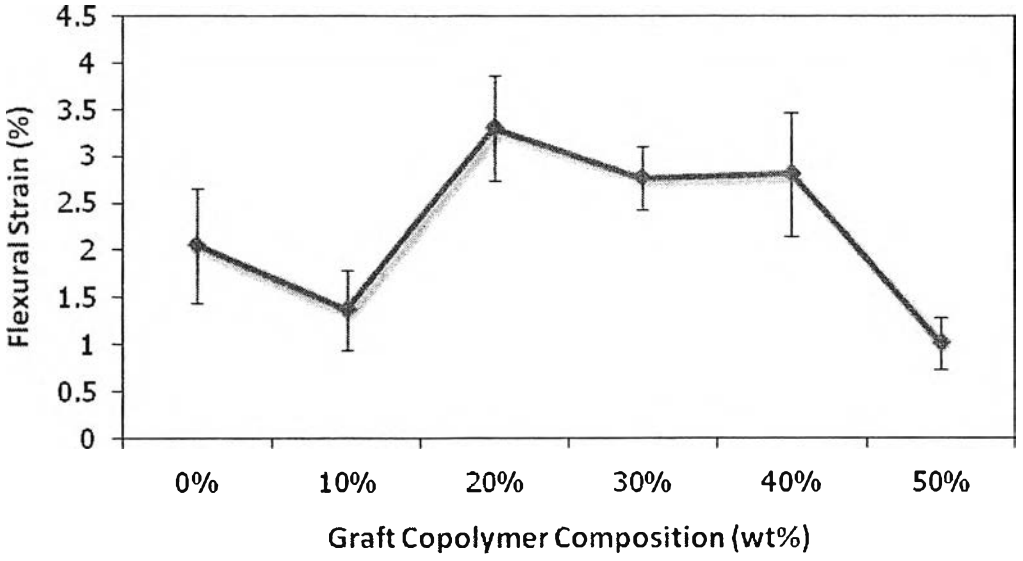

Figure 5.15 Flexural strain of the biocomposites as a function of a graft copolymer content as obtained from the 3-point bending experiments. Flexural strain of the polybenzoxazine is also noted for comparison.

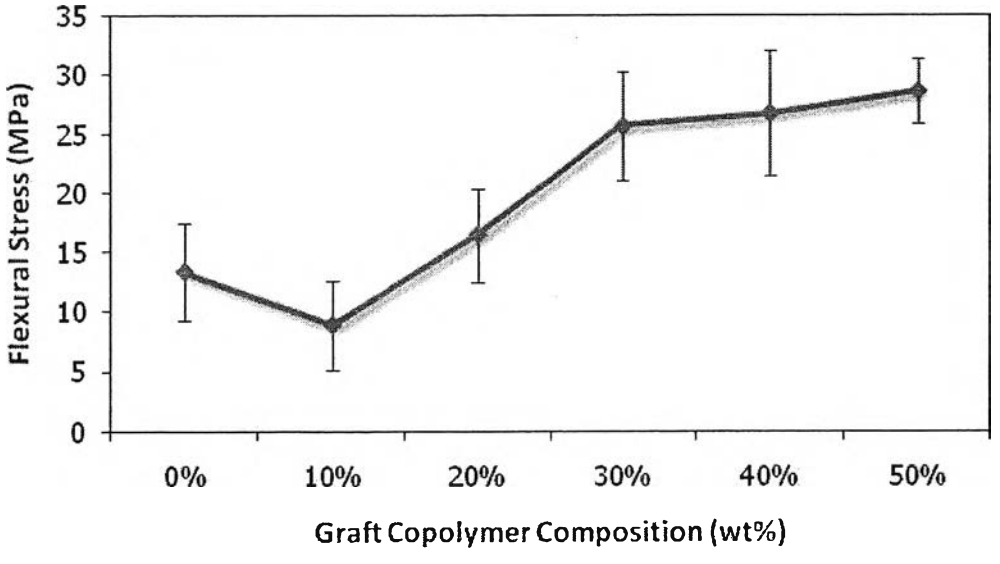

Figure 5.16 Flexural stress of the biocomposites as a function of a graft copolymer content as obtained from the 3-point bending experiments. Flexural stress of the polybenzoxazine is also noted for comparison.

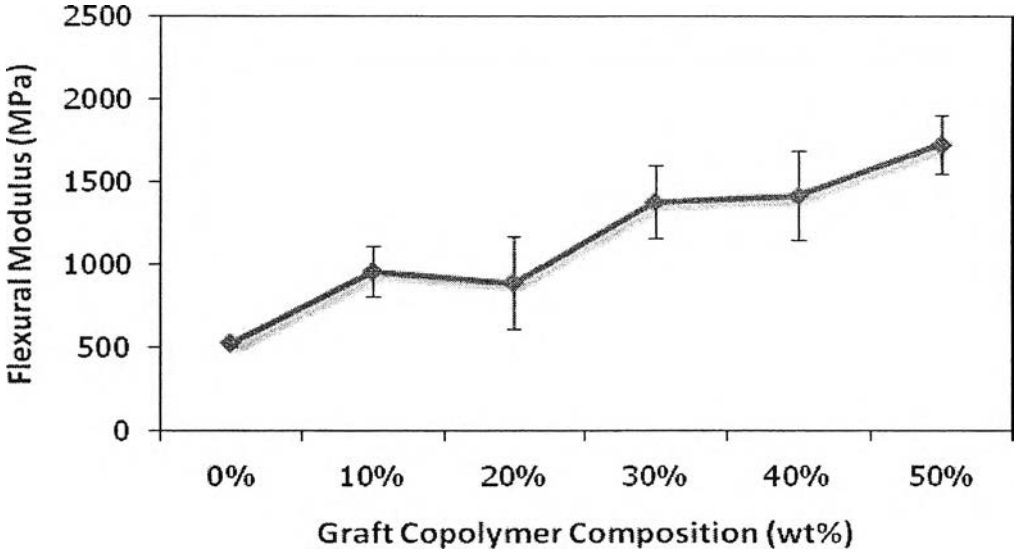

Figure 5.17 Flexural moduli of the biocomposites as a function of a graft copolymer content as obtained from the 3-point bending experiments. Flexural modulus of the polybenzoxazine is also noted for comparison.

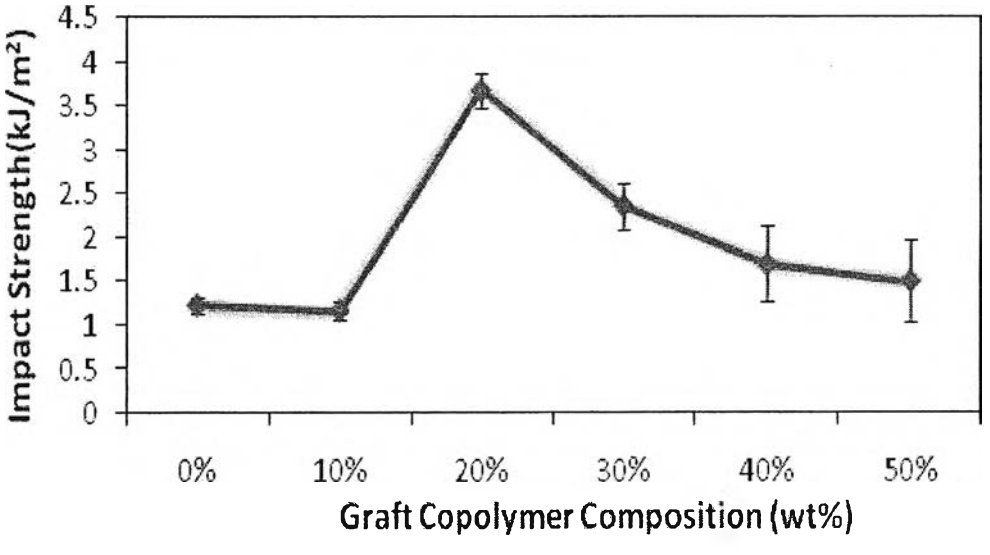

Figure 5.18 Impact strength of the biocomposites as a function of a graft copolymer content as obtained from the ZWICK impact testing. Impact strength of the polybenzoxazine is also noted for comparison.

Typical polybenzoxazine shows high stress at yield and modulus, but the poor toughness makes it easy to break. The incorporation between modified-surface marl filled graft copolymer with PBZ did not have a significant influence on the flexural strain of the biocomposites. When adding graft copolymer-marl from 10–20 wt%, the flexural strain was increasing too. But after that concentration the flexural strain of the biocomposites shows a decreasing trend like the marl–PBZ composites when increasing load of the filler. Atikler *et al.,* 2006 explained that this decreasing trend was occurred by stress concentrations that initiate cracks around filler particles and there was some filler agglomeration revealed by SEM at the high concentration of graft copolymer-marl in polybenzoxazine composite, so after that point the flexibility would be lost. Whereas the flexural stress of the biocomposites tended to increase with an increasing of graft copolymer contents since a thermoplastic parts can absorb the loaded stress. The elastic modulus of the biocomposites is reduced when adding 10 wt% graft copolymer-marl and turns to increase with graft copolymer-marl loading beyond 10 wt%. The increasing stress and modulus are explained by the high curing content of PBZ (e.g. at 30 wt%, which the flexural modulus of graft copolymer-marl biocomposite is high comparable to that of silane treated-$CaCO_3$ polypropylene composite, Leong *et al.,* 2005) and the more rigidity arisen with the higher content of marl filler (see Table 5.5).

In opposite to the flexural test, the impact strength tends to increase with increasing the biocomposite content from 10 to 30 wt%, and drops after increasing loading content. This suggests that the incorporated graft copolymer-marl provide better absorption of the impact energy for PBZ. When comparing from 0 to 50 wt% of graft copolymer content in the polybenzoxazine composite, the ratio of 20/80 and 30/70 wt% of graft copolymer filled with amino silane treated-surface marl biocomposites/PBZ showed the optimum values of both flexural properties and impact strength. And the 20 wt% ser-g-PLA and silane trated marl showed the highest flexural strain and impact strength at the acceptable flexural modulus comparing with preferred splint material properties in patent application 20070016323 (more than 13.4 MPa at 23°C). The improved mechanical properties also suggest that these blends are compatible and Ser-g-PLA/marl biocomposites can effectively enhance toughness of polybenzoxazine 2–3 times.

5.4.4.4 The Dynamic Mechanical Analysis of the Biocomposites

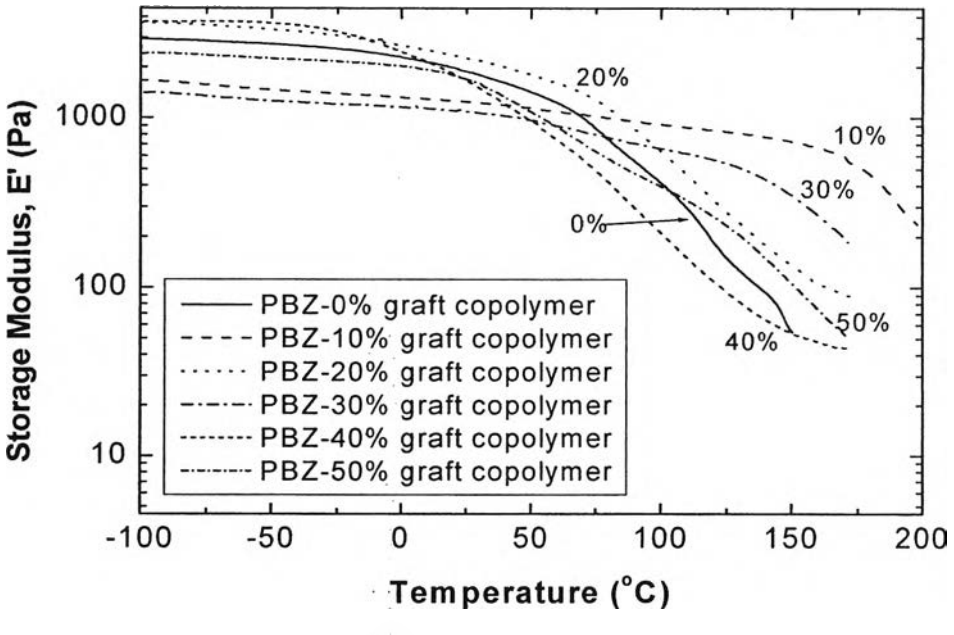

Figure 5.19 Storage moduli for the synthesized polybenzoxazine and biocomposites (from 10 to 50 wt% graft copolymer contents).

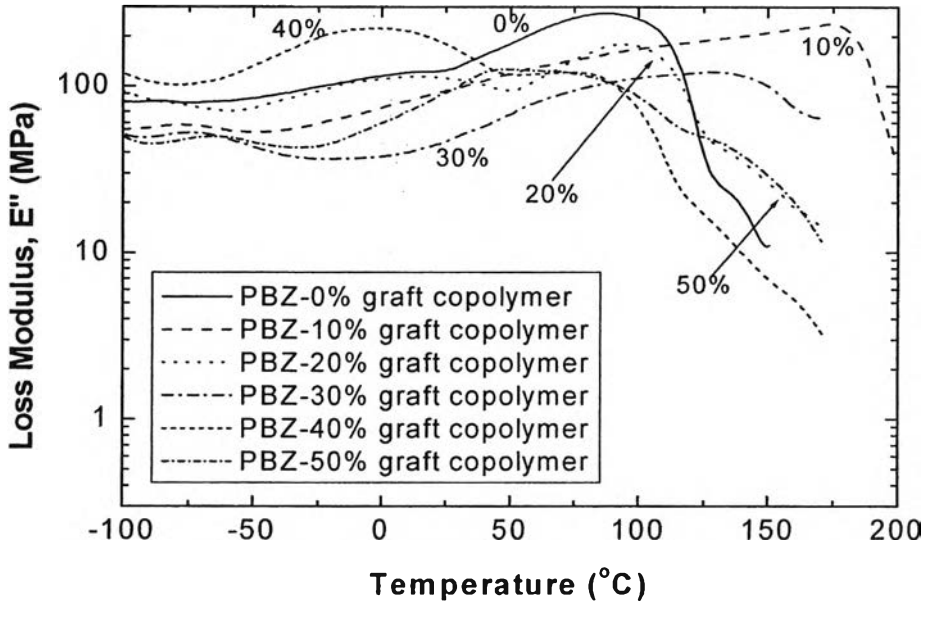

Figure 5.20 Loss moduli for the synthesized polybenzoxazine and biocomposites (from 10 to 50 wt% graft copolymer contents).

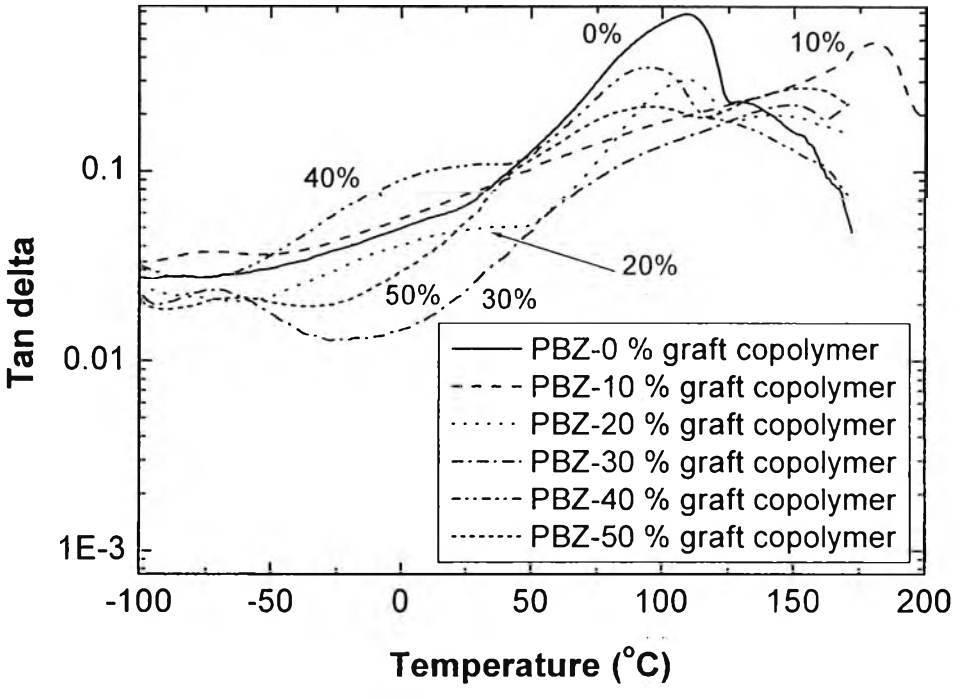

Figure 5.21 Tan δ curves for the synthesized polybenzoxazine and biocomposites (from 10 to 50 wt% graft copolymer contents).

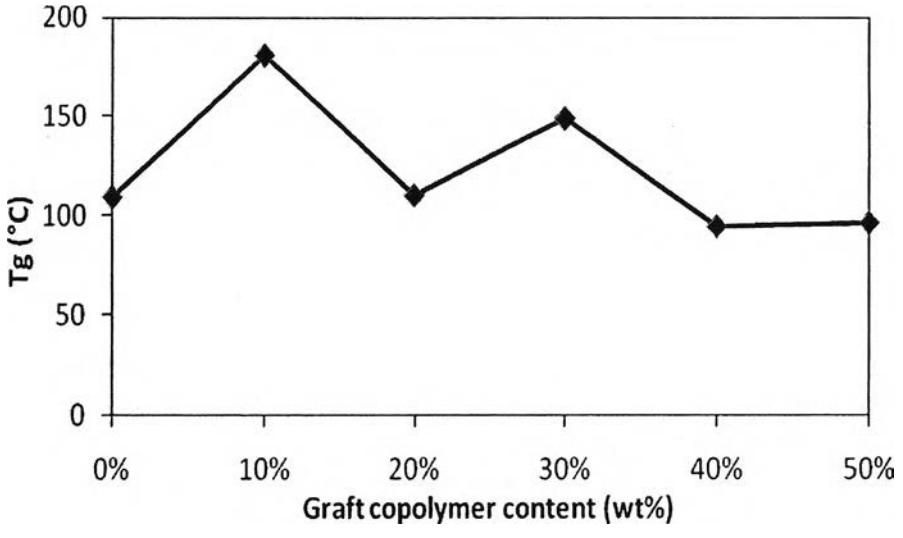

Figure 5.22 Glass transition temperature of the biocomposites from the maximum of tan δ peak as a function of graft copolymer contents in the composites.

The dynamic mechanical properties of the biocomposites were measured over the temperature range from -100°C to beyond the glass transition temperature (T_g) of each material. The elastic or storage modulus of a solid sample at room temperature, E′, provides a measurement of the material stiffness, which related to changes in the stored elastic energy under a deformation process as the molecular segments resist motion (Epinosa *et al.*,2003), is depicted in Figure 5.19. The modulus was highest when adding 40 wt% graft copolymer and there was no clear trend due to the voids generated during compression process.

T_g of the materials is allowed to determined by DMA. It is detected at the maximum of the loss modulus which corresponds to the initial drop from the glassy state into the transition. The loss modulus spectrum or viscous component, E″, for each biocomposite materials as the function of temperature is shown in Figure 5.20. The broadening of the E″ peak after incorporation with graft copolymer indicates an increase in the number of modes of branching or shows a higher degree of crosslinking from the interaction between graft copolymer and polybenzoxazine, which results in a wider distribution of structure or lower segmental mobility and fewer relaxing species (Huang *et al.*, 2005).

Additionally, the tan δ of composites with different contents of graft copolymer is shown in the Figure 5.21. These tan δ curves can determined the main α-relaxation process of the loss factor associated with the glass to rubber transition for each of the benzoxazine composites (T_g) and related to the transition midpoint of the log of the storage modulus (E′) curve. Moreover, all curves of tan δ reveal that these blends are compatible. The values of glass transition temperature of each material from both measurements showed the decreasing trend upon increasing the graft copolymer contents from 10 to 50 wt% or on the opposite way for the storage modulus. From results in Figure 5.22 the glass transition temperature from the maximum of tan δ peaks are approximately 181, 110, 149, 94, and 96 °C for 10–50 wt% graft copolymer contents respectively. Because the glass transition process is related to the molecular motion, so the value of glass transition temperature is corresponding to the molecular packing and the chain rigidity and linearity. Therefore, the results of T_g when introduction of the 10–30 wt% graft copolymer into PBZ, which was signifi-

cantly higher than 109 °C of pure synthesized polybenzoxazine, imply that the rigidity of the biocomposite was improved compared to that of polybenzoxazine, whereas the content of graft copolymer beyond 30 wt% will reduce the rigidity of products.

5.5 CONCLUSIONS

The graft copolymer of silk sericin protein and PLA was synthesized by in-situ catalytic bulk polymerization in the presence of marl and stannous octoate by melt mixing. The obtained marl filled graft copolymer was further blended with benzoxazine precursor, which can be synthesized via a faster quasi-solventless method, and cured stepwise to obtain a biocomposite hardened by PBZ. The resulting of grafting-from structure and PBZ preparation were investigated by FTIR, NMR, and thermal analysis. From DSC curves and XRD patterns, the graft copolymer showed no crystal structure indicating that the high efficiency of grafting obstructed the crystallization. However the biocomposites obtained from modified-surface marl filled graft copolymer blended with PBZ exhibited comparable thermal properties to PBZ–marl composites, namely, the marl-filled composites had the lower curing temperature and the higher thermal stability than the pure PBZ. This effect was explained by the presence of silica in marl which can act as an acid catalyst. The mechanical properties after introducing graft copolymer into PBZ matrix were poorer than pure PBZ at low loading but at high loading of graft copolymer (30–50 wt%), the flexural strength at yield and modulus of the biocomposites were greatly improved. The overall impact strength of the biocomposites was higher than that of the pure polybenzoxazaine because the incorporated graft copolymer can absorb the loaded strength. Among the five ratios of the biocomposite done in this research, the 20 wt% of graft copolymer filled with amino silane treated-surface marl biocomposite by PBZ showed the highest values of the flexural strain and the impact strength, which are the preferrable properties for soft splint application. In addition, the DMA results showed that each glass-transition temperature of the biocomposite was comparable or higher in comparison with purely synthesized PBZ.

5.6 ACKNOWLEDGEMENTS

The authors would like to thank to Chul Thai Silk Co., Ltd. for the supply of sericin powder, Mettler Toledo Co., Ltd. for the thermal properties measurement and also to the Ratchadapiseksompoch Endowment and Center of Excellence for Petroleum, Petrochemicals, and Advanced Materials, Chulalongkorn University, Thailand, for the financial support. The authors would also thanks the National Research Council of Thailand (NRCT) for graduate research assistant scholarship.

5.7 REFERENCES

[1] Agag, T., and Takeichi, T. (2007) High-Molecular-Weight AB-Type Benzoxazine as New Precursors for High-Performance Thermosets. Journal of Polymer Science: Part A: Polymer Chemistry , 46, 1878–1888.

[2] Allen, D., and Ishida, H. (2006) Physical and Mechanical Properties of Flexible Polybenzoxazine Resins: Effect of Aliphatic Diamine Chain Length Journal of Applied Polymer Science, 101, 2798–2809.

[3] Altikler, U., Basalp, D., and Tihminlioglu, F. (2006) Mechanical and Morphological Properties of Recycled High-Density Polyethylene, Filled with Calcium Carbonate and Fly Ash. Journal of Applied Polymer Science, 120, 4460-4467.

[4] Cai, Q., Wan, Y., Bei, J., and Wang, S. (2003) Synthesis and characterization of biodegradable polylactide-grafted dextran and its application as compatilizer. Biomaterials., 24, 3555–3562.

[5] Cho, K.Y., Moon, J.Y., Lee, Y.W., Lee, K.G., Yeo, J.H., Kweon, H.Y., Kim, K.H., and Cho, C.S. (2003) Preparation of self-assembled silk sericin nanoparticles. International Journal of Biological Macromolecules, 32, 36–42.

[6] Christos, G.K., and Nikos, V.V. (2000) Calcium Carbonate Phase Analysis Using XRD and FT-Raman Spectroscopy. Analyst, 125, 251–255.

[7] Dieter, B. (1997) Chemical synthesis of polylactide and its copolymers for medical applications. Polymer Degradation and Stability, 59, 129–135

[8] Dash, R., Mukherjee, S., and Kundu, S.C. (2006) Isolation, purification and characterization of silk protein sericin from cocoon peduncles of tropical tasar silkworm, *Antheraea mylitta*. International Journal of Biologiacl Macromolecules, 38, 255–258.

[9] Dash, R., Ghosh, S.K., Kaplan, L.D., and Kundu, S.C. (2007) Purification and biochemical characterization of a 70 kDa sericin from tropical tasar silkworm, *Antheraea mylitta*. Comparative Biochemistry and Physiology, 147, 129–134.

[10] Dong, H., Xu, Q., Li, Y., Mo, S., Cai S., and Liu, L. (2008) The synthesis of biodegradable graft copolymer cellulose-*graft*-poly(l-lactide) and the study of its controlled drug release. Colloids and Surfaces B: Biointerfaces, 66, 26–33.

[11] Espinosa, M.A., Cadiz, V., and Galia, M. (2003) Synthsis and Characterization of Benzoxazine-Based Phenolic Resins: Crosslinking Study. Journal of Applied Polymer Science, 90, 470–481.

[12] Fried, S., and Valley, G. (2006) Splint and or method of making same. United States Patent, Patent number 0,016,323.

[13] Ghosh, N.N., Kiskan, B., and Yagci, Y. (2007) Polybenzoxazines—New high performance thermosetting resins: Synthesis and properties. Prog. Polym. Sci., 32, 1344–1391.

[14] Gong, Q., Wang, L., and Tu, K. (2006) In situ polymerization of starch with lactic acid in aqueous solutionand the microstructure characterization. Carbohydrate Polymers, 64, 501–509.

[15] Hyon, S.H., Jamshidi, K., and Ikada, Y. (1997) Synthesis of polylactides with different molecular weights. Biomaterials, 18, 1503–1508.

[16] Huang, J.-M., amd Yang S.-J. (2005) Studying the miscibility and thermal behavior of polybenzoxa zine/ poly(ε-caprolactone) blends using DSC, DMA, and solid state ^{13}C NMR spectroscopy. Polymer, 46(19) 8068–8078.

[17] Ishida, H., and Lee, Y.H. (2001) Synergism observed in polybenzoxazine and poly(ε-caprolactone) blends by dynamic mechanical and thermogravimetric analysis. Polymer, 42(16) 6971–6979.

[18] Ishida, H., and Lee, H. (2001) Study of hydrogen bonding and thermal properties of polybenzoxazine and poly-(ε-caprolactone) blends. Journal of Polymer Science Part B: Polymer Physics, 39(7) 736–749.

[19] Ishida, H., and Low, H. (1998) Synthesis of Benzoxazine Functional Silane and Adhesion Properties of Glass-Fiber-Reinforced Polybenzoxazine Composites Journal of Applied Polymer Science, 69, 2559–2567.

[20] Jacobsen, S., Fritz, H.G., Degee, Ph., Dubois, Ph., and Jerome, R. (2000) Single-step reactive extrusion of PPLA in a corotating twin-screw extruder promoted by 2-ethylhexanoic acid tin(II) salt and triphenylphosphine. Polymer, 41, 3395–3403.

[21] Jacobsen, S., Fritz, H.G., Degee, Ph., Dubois, Ph., and Jerome, R. (2000) New developments on the ring opening polymerization of polylactide. Industrial Crops and Products, 11, 265–275.

[22] Janata, M., Masar, B., Toman, L., Vlcek, P., Latalova, P., Brus, J., and Holler, P. (2003) Synthesis of novel types of graft copolymers by a "grafting-from" method using ring-opening polymerization of lactones and lactides. Reactive & Functional Polymers, 57, 137–146.

[23] Jin, S., and Gonsalves, K.E. (1997) Synthesis of poly(l-lactide-co-serine) and its graft copolymers with poly(ethylene glycol). Polymer, 39, 5155–5162.

[24] Jiang, L., Zhang, J., and Wolcott, M. (2007) Comparison of polylactide/nano-sized calcium carbonateand polylactide/montmorillonite composites: Reinforcing effects and toughening mechanisms. Polymer, 48, 7632–7644.

[25] Kaplan, D.L. (1998) Biopolymers from Renewable Resources. New York: Springer.

[26] Kiskan, B., and Yagci, Y. (2005) Synthesis and characterization of naphthoxazine functional poly(ε-caprolactone). Polymer, 46, 11690–11697.

[27] Kowalski, A., Duda, A., and Penczek, S. (2000) Kinetics and Mechanism of Cyclic esters Polymerization Initiated with Tin(II) Octoate. Macromolecules, 33, 7359–7370.

[28] Lamoolphak, W., De-Eknamkul, W., Shotipruk, A. (2008) Hydrothermal production and characterization of protein and amino acids from silk waste. Bioresource Technology, 99(16), 7678-7685.

[29] Lee, S., Miyazaki, K., Hisada, K., and Hori, T. (2004) Application of silk Sericin to Finizhing of Synthetic Fabric. Gakkaishi, 60, No.1, 43–49.

[30] Leong, Y., Bakar, M., Ishak, Z., and Ariffin, A. (2005) Effects of Filler Treatments on the Mechanical, Flow, Thermal, and Morphological Properties of Talc and Calcium Carbonate Filled Polypropylene Hybrid Composites Journal of Applied Polymer Science, 98, 413–426.

[31] Liu, Y., Tian, F., and Hu, K.A. (2004) Synthesis and characterization of a brush-like copolymer of polylactide grafted onto chitasan. Carbohydrate Research, 339, 845–851.

[32] Luckachan, G., and Pillai, C.K.S. (2006) Chitosan/oligo L-lactide graft copolymers: Effect of hydrophobic side chains on the physico-chemical properties and biodegradability. Carbohydrate Polymers, 64, 254–266.

[33] Marcelino, L., Gimenes, Li, L., and Xianshe, F. (2007) Sericin/poly(vinyl alcohol) blend membranes for pervaporation separation of ethanol/water mixtures. Journal of Membrane Science, 295 , 71–79.

[34] Mondal, M., Trivedy, K., and Nirmal Kumar, S. (2007) The Silk proteins, sericin and fibroin in silkworm, Bombyx mori Linn., - a review. Caspian J. Env. Sci. , Vol.5 No.2, 63–76.

[35] Nakatsuka, T., Kawasaki, H., and Itadani, K. (1979) Functional Silane-Modified Calcium Carbonate Journal of Applied Polymer Science, 4, 1985–1995.

[36] Nichakarn, K., and Magaraphan, R. (2007) High Dieletric Composite Material at Multi-frequency Range. M.S. Thesis. The Petroleum and Petrochemical College. Chulalongkorn.

[37] Patcharakamon, N., Ishida, H., and Hathaikarn, M (2007) The Catalytic Extrusion of Polylactide/Ethylene Vinyl Alcohol Bioplastic Film. M.S. Thesis. The Petroleum and Petrochemical College. Chulalongkorn.

[38] Phiriyawirut, P., Magaraphan, R., and Ishida, H. (2001) Preparation and characterization of polybenzoxazine-clay immiscible nanocomposite. Mat Res Innovat, 4, 187–196.

[39] Sarovart, S., Sudatis, B., Meesilpa, P., Grady, B., and Magaraphan, R. (2003) The use of sericin as an antioxidant and antimicrobial for polluted air treatment. Rev.Adv.Mater.Sci., 5, 193–198.

[40] Sodergard, A., and Stolt, M. (2002) Porperties of lactic acid based polymers and their correlation with composition. Prog. Polym. Sci., 27, 1123-1163.

[41] Sorina-Alexandra, G., Horia, I., Alina, N., and Calin, D. (2007) Thermal Polymerization of Benxozazine Monomers Followed by GPC, FTIR and DETA. Polymer testing, 26, 162-171.

[42] Su, Y., Chen, W., Ou, K., and Chang, F. (2005) Study of the morphologies and dielectric constants of nanoporous materials derived from benzoxazine-terminate poly(ε-caprolactone)/polybenzoxazine co-polymers. Polymer, 46, 3758–3766.

[43] Takeichi, T., Takuya, K., and Tarek, A. (2005) Synthesis and thermal cure of high molecular weight polybenzoxazine precursors and the properties of the thermosets. Polymer , 46, 12172–12180.

[44] Teramoto, H., Nakajima, K., and Takabayashi, C. (2004) Chemical Modification of Silk Sericin in Lithium Chloride/Dimethyl Sulfoxide Solvent with 4-Cyanophenyl Isocyanate. Biomacromolecules, 5, 1392–1398.

[45] Wang, Y.-X., and Ishida, H. (1999) Cationic ring-opening polymerization of benzoxazines. Polymer, 40, 4563–4570.

[46] Wang, Y., and Lee, W. (2003) Interfacial Interactions in Calcium Carbonate-Polypropylene Composites. 1: Surface Characterization and Treatment of Calcium Carbonate: A Comparative Study Polymer Composites, 24(1), 119–131.

[47] Wu, J., Wang, Z., and Xu, S. (2007) Preparation and characterization of sericin powder extracted from silk industry wastewater. Food Chemistry, 103, 1255–1262.

[48] Wu, Y., Zheng, Y., Yang, W., Wang, C., Hu, J., and Fu, S. (2005) Synthesis and Characterization of a novel amphiphilic chitosan-polylactide graft copolymer. Carbohydrate Polymers, 59, 165–171.

[49] Zhang, Y. (2002) Application of natural silk protein sericin in biomaterails. Biotechnology Advances , 20, 91–100.